



Received: 25-11-2013
Accepted: 18-12-2013

ISSN: 2321-4902
Volume 1 Issue 4



Online Available at www.chemijournal.com

International Journal of Chemical Studies

Miscibility, Conductivity and Dielectric Studies of Poly (methyl methacrylate) and Cellulose acetate propionate Blends

Denthaje Krishna Bhat^{1*}, H.S. Sreekantha Jois¹

1. Department of Chemistry, National Institute of Technology Karnataka, Surathkal, Srinivasnagar-575025, India.

*[Email: denthajekb@gmail.com, +91 824 2473202]

In the present era, material scientists are focusing on polymer blends with good miscibility and conductivity. Accordingly we report here, polymer blends of Poly (methyl methacrylate) and Cellulose acetate propionate of varying blend compositions prepared by solution casting method. The miscibility, water uptake, ion exchange capacity, proton conductivity and dielectric behavior of these blends have also been studied. The proton conductivity of the blends was found to be in the order of 10^{-3} S cm^{-1} . Dimethyl formamide has been used as solvent. Fourier transform infrared spectra and differential scanning calorimetry measurements have been used to analyze the miscibility of the blends. Up to a PMMA:CAP composition of 50:50, water uptake amount of the blends showed an increasing trend. Combination of the results suggested that the variations in associated properties are due to intermolecular hydrogen bonding interaction between hydroxyl and carbonyl groups of CAP and PMMA respectively.

Keyword: Polymer blends, Glass Transition, Miscibility, Conductivity, PMMA.

1. Introduction

Polymer blending is a convenient technique for designing materials with tailored properties without synthesizing totally new materials. Polymer blends exhibit superior properties compared to that of individual component polymer. The main advantages of the blend systems are simplicity of preparation, inexpensiveness and ease of control of physical properties by compositional change. The property modification of the polymer is believed to depend on the miscibility of the polymer pair used in blending^[4]. Polymer-polymer miscibility has been widely studied in the polymer literature. Such studies have great significance for engineering applications of polymers^[5].

The miscibility of polymer blends is generally believed to originate from the specific interactions between polymers. Thermodynamically, the presence of hydrogen-

bonding interactions between proton donor and acceptor polymers can improve the miscibility of their blends^[6, 7]. There are numerous techniques to study the miscibility of the polymer blends. The most useful techniques are thermal analysis and spectroscopy. To investigate the miscibility of polymer blends, Differential Scanning Calorimetry (DSC) has been frequently used in order to determine the glass transition temperature (T_g). A single glass transition will indicate the miscibility of two polymer components. FT-IR spectroscopy is another method to determine the polymer miscibility and is used to elucidate the interactions present in blends^[8].

Poly (methyl methacrylate) (PMMA) is a non-biodegradable polymer with good transparency, mechanical strength, less weight, chemical resistance, colorlessness, resistance to weathering corrosion and good insulating properties. PMMA

is the most commonly used polymer among the methacrylate family and has found tremendous applications in automotive and home appliances. Cellulose esters, prime among them, Cellulose Acetate Propionate (CAP) is one of the most important derived natural polymers and hence can be susceptible to biodegradation. Cellulose esters are used in miscible blends with acrylics, polyesters and other polymers because of their ability to form hydrogen bonds through the presence of hydroxyl groups and the carboxyl groups of the ester. Therefore, the polymer blends of PMMA and CAP can make suitable materials for many key applications where biodegradation is desirable. Hence it is of interest to study the properties of these blends. In view of this and as a part of our ongoing research work on polymer blends and composites [9-15], polyblends of PMMA and CAP have been prepared by solution casting method. FTIR-ATR and DSC have been used to analyze the miscibility and existence of specific interactions in the blends. The water uptake, ion-exchange capacity and proton conductivity behavior of the blends have also been studied.

2. Experimental

2.1 Materials

Polymers tested in this work were obtained from commercial sources and were used as received. PMMA, with MW=1,20,000 and CAP, with MN = 75,000 were supplied by Sigma Aldrich. Dimethyl formamide (DMF) was used as solvent.

2.2 Preparation of blends

Blends of PMMA with CAP were prepared by solution casting. The % (w/v) stock solutions of PMMA and CAP were prepared in DMF by stirring for 24 hours. The solution mixtures thus prepared were stirred for three hours for uniform mixing. They were then poured into Teflon petri dishes and the solvent was allowed to evaporate at 60 °C for 72 h in a vacuum oven. The dried films were taken out and stored in a vacuum desiccator.

3. Membrane characterization

3.1 Fourier transform infrared (FTIR) spectroscopic studies

FTIR spectra of the PMMA, CAP and PMMA/CAP blends were scanned in the range between 4000 and 400 cm^{-1} on a NICOLET AVATAR 330 FTIR-ATR spectrophotometer with resolution of 4.000 cm^{-1} .

3.2 Differential scanning calorimetry (DSC) Studies

DSC thermograms of PMMA, CAP and PMMA/CAP blends were obtained on a SHIMADZU DSC-60. The sample of 4 to 4.5 mg in weight was sealed in an aluminium pan and measurements were performed over the temperature range of ambient to 250 °C at the heating rate of 10 °C min^{-1} under nitrogen gas flow.

3.3 Water uptake

The water uptake in the PMMA/CAP blends was measured by immersing the blends into deionized water at room temperature for 24 h. Then the blends were taken out, gently pressed between the folds of the tissue paper and immediately weighed on a balance. Triplicates were run for each blend to get the satisfactory reproducibility [11]. The water uptake in the blends, W , was calculated by using Equation (1).

$$W = \frac{W_{wet} - W_{dry}}{W_{dry}} \quad (1)$$

where, W_{dry} and W_{wet} are the weight of dry and corresponding water absorbed membranes, respectively.

3.4 Ion exchange capacity measurements

Ion exchange capacity (IEC) indicates the number of milliequivalents (mequiv.) of ions in 1 g of the dry polymer blend. To determine the ion exchange capacity, blends of similar weight were soaked in 50 mL of 0.01 N sodium hydroxide (NaOH) solution for 24 h at ambient temperature. After 24 h, 10 mL of the solution was titrated with 0.01 N sulphuric acid (H_2SO_4), using a

phenolphthalein indicator. IEC was calculated by using Equation (2).

$$IEC = \frac{(B - P) \times 0.01 \times 5}{m} \quad (2)$$

where, IEC is ion exchange capacity (in mequiv g^{-1}), B is amount of H_2SO_4 used to neutralize blank sample solution in mL. P is amount of H_2SO_4 used to neutralize the blend soaked solution used in the study in mL, 0.01 is normality of the H_2SO_4 . Here, 5 is the factor corresponding to the ratio of the amount of NaOH used to soak the blend/s to the amount used for titration and m is the mass of the polymer blend in g [16].

3.5 Electrochemical impedance spectroscopy and proton conductivity measurement

The AC impedance spectra of the membranes were recorded in the frequency range between 0.01 Hz and 100000 Hz with amplitude of 5 mV using AUTOLAB Electrochemical System (Eco Chemie BV, Netherlands) over the temperature range of 30 °C to 70 °C. Proton conductivity measurements were performed on the membranes in a typical two-electrode cell by AC impedance technique. The conductivity cell composed of two copper electrodes of 2 cm \times 2 cm dimensions. The blend sample was sandwiched between the two copper electrodes fixed in a Teflon block and kept in a closed glass container. 1 M NaCl solution was used as an electrolyte. The cell was kept at each measuring temperature for a minimum of 60 min to ensure thermal equilibration of the sample at the temperature before measurement. The resistance value associated with the blend conductivity was determined from the high frequency intercept of the impedance with the real axis. The blend conductivity was calculated from the membrane resistance, R , using the following Equation (3):

$$\sigma = L/RA \quad (3)$$

where, σ is the proton conductivity of blend (in S cm^{-1}), L is the thickness (in cm) and A is the area of the blend (in cm^2).

3.6 Dielectric studies

Complex impedance data, Z^* can be represented by its real, Z_R and imaginary, Z_I parts by the relation:

$$Z^* = Z_R + jZ_I \quad (4)$$

The relationships between complex impedance, admittance, permittivity and electrical modulus can be found elsewhere [13].

The equations for the dielectric constant, ϵ_R and the dielectric loss, ϵ_I , can be shown as

$$\epsilon_R = \frac{Z_I}{\omega C_0 (Z_R^2 + Z_I^2)} \quad (5)$$

$$\epsilon_I = \frac{Z_R}{\omega C_0 (Z_R^2 + Z_I^2)} \quad (6)$$

Here $C_0 = \frac{\epsilon_0 A}{t}$ and ϵ_0 is the permittivity of the free space, A is the electrolyte-electrode contact area and t is the thickness of the sample and $\omega = 2\pi f$, f being the frequency in Hz.

4. Results and Discussion

4.1 FTIR spectroscopic studies

The presence of hydrogen bonding and the miscibility of the blends in the solid state are determined using the FTIR spectroscopy. The magnitude of the bond lengths and electron densities associated with the formation of hydrogen bonds are actually quite small when compared with the typical chemical changes and changes in energies. However, FTIR spectroscopy is very sensitive to detect the formation of the hydrogen bond [17].

In general, when hydrogen bond formation occurs between two groups, the vibration frequencies of both the groups are expected to show a red shift compared with the free non-interacting group frequencies. A polymer blend made of polymers consisting of carbonyl and hydroxyl moieties as in the present case where PMMA has carbonyl group and the CAP has both the carbonyl and hydroxyl groups is also expected to show a red shift compared with the free non-interacting

group frequencies. FTIR spectra of pure PMMA, PMMA/CAP 50/50 blend and pure CAP were shown in Figure 1 (a,b,c) respectively.

The carbonyl frequency of pure CAP (Figure 1 (c)) at 1736.7 cm^{-1} decreased to 1725.7 cm^{-1} in the PMMA/CAP 50/50 blend (Figure 1 (b)), showing the formation of a weak hydrogen bond between component polymers in the blend. This can be contributing to the miscibility of the blends. The strong and broad band at around

3483.0 cm^{-1} in pure CAP and 3616.4 cm^{-1} in PMMA/CAP 50/50 blend corresponded to the -OH stretching vibrations of hydroxyl groups. The indication that part of the -OH groups were involved in the hydrogen bond formation shows that the intensity of the broad band is decreased after blending. These results indicate that the forces that exist in the blends may be due to the weak hydrogen bonding interactions.

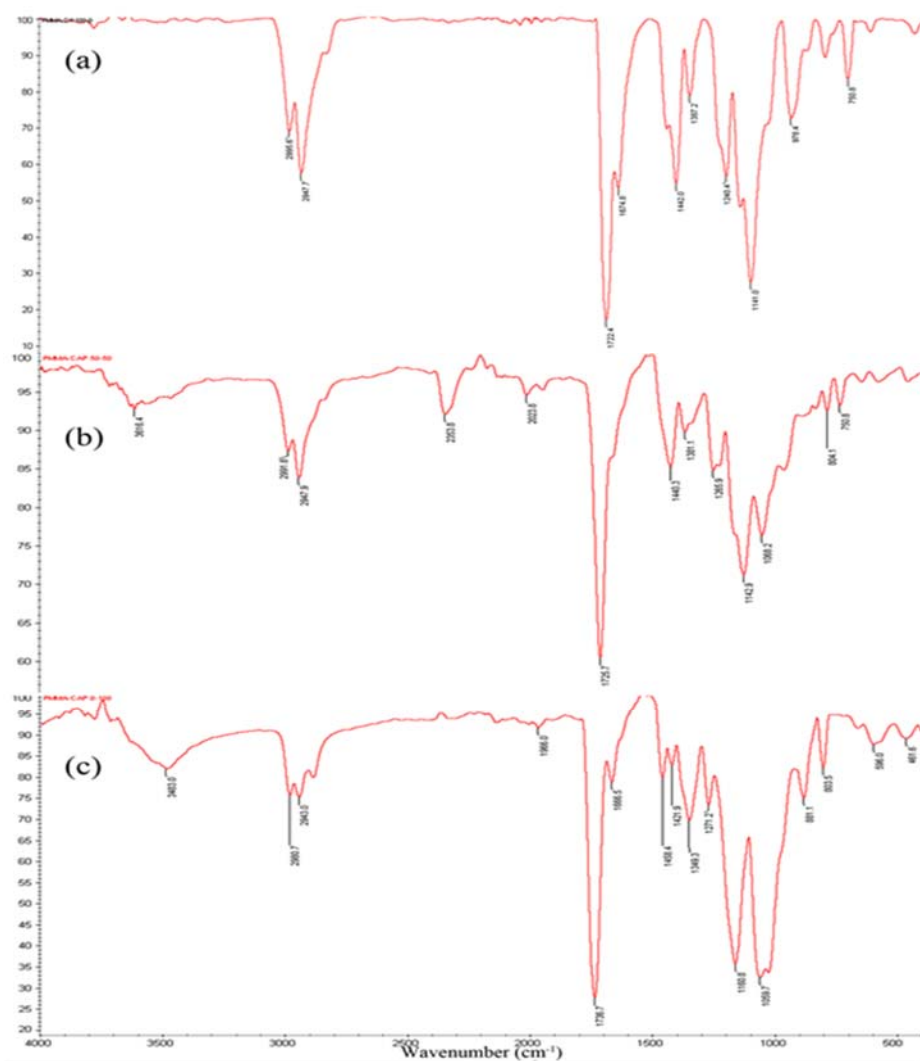


Fig 1(a, b, c): FTIR spectra of pure PMMA, PMMA/CAP 50/50 blend and pure CAP.

4.2 DSC Studies

The literature discusses the Miscibility of blends extensively. The miscibility of the polymer blends can be comprehended by utilizing DSC,

one of the standard methods. The DSC thermograms of pure PMMA, pure CAP and PMMA/CAP blends are shown in Figure 2 (a) and Figure 2 (b) respectively.

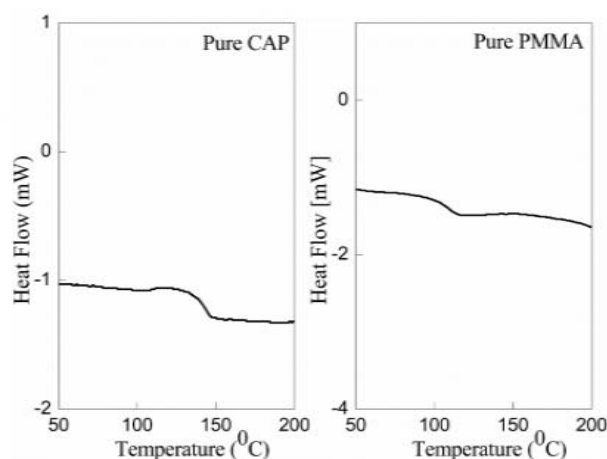


Fig 2(a): DSC scans of pure PMMA and pure CAP.

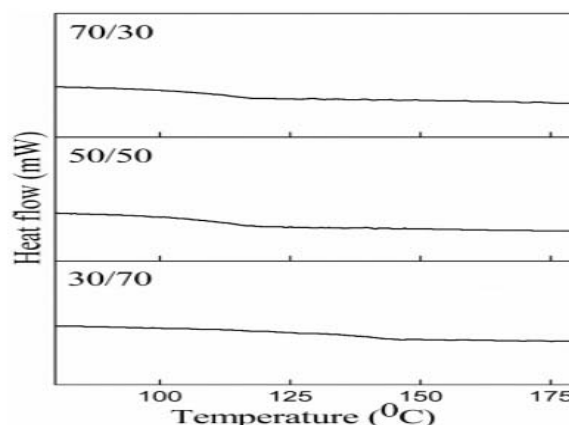


Fig 2(b): DSC scans of PMMA/CAP 50/50 blend.

From Figure 2(a), it can be seen that the T_g for pure CAP is 141.8 °C and PMMA is 107.5 °C. It is interesting to note here that the thermograms for the blends (Figure 2 (b)) exhibited single T_g and its value lies in-between T_g values of pure PMMA and pure CAP. Further, the T_g values of the blend films decreased with the increase of PMMA content in the blends. Such a systematic variation of T_g in the blends is indicative of miscibility of the components in the blends. The glass transition temperature of the blend films from the properties of the pure elements can be estimated using many theoretical equations. Gordon-Taylor equation^[18,19] (Equation (7)) and Fox equation^[10,20] (Equation (8)) are the frequently used expressions for predicting the glass transition temperature of amorphous polymer blends:

$$T_g^b = \frac{W_1 T_{g1} + k W_2 T_{g2}}{W_1 + k W_2} \quad (7)$$

$$\frac{1}{T_g^b} = \frac{W_1}{T_{g1}} + \frac{W_2}{T_{g2}} \quad (8)$$

where, T_g^b is glass transition temperature (T_g) of the blend, T_{g1} and T_{g2} are the glass transition temperatures of the pure components, PMMA and CAP respectively. W_1 and W_2 are weight fraction of components, PMMA and CAP respectively. k is a fitting parameter and the experimental data is best fitted by this equation with $k=0.76$. This result supports that PMMA/CAP blends have high miscibility in the amorphous state. The thermal properties of PMMA/CAP blends are represented in Table 1.

Table 1: Thermal properties of PMMA/CA blends.

Sample	PMMA (wt %)	T _g (°C)	Fox equation	Gordon-Taylor equation
0/100	0	141.80	141.80	141.80
10/90	10	140.99	137.41	137.42
20/80	20	139.66	133.28	133.30
30/70	30	138.67	129.39	129.42
40/60	40	134.65	125.73	125.75
50/50	50	118.91	122.26	122.29
60/40	60	113.74	118.97	119.01
70/30	70	112.33	115.88	115.89
80/20	80	112.15	112.93	112.94
90/10	90	111.17	110.13	110.13
100/0	100	107.46	107.46	107.46

The blends show a positive deviation from Fox equation implying an intermolecular interaction between the polymers.

4.3 Water uptake

Figure 3 shows the relationship between water uptake and PMMA content in the blends.

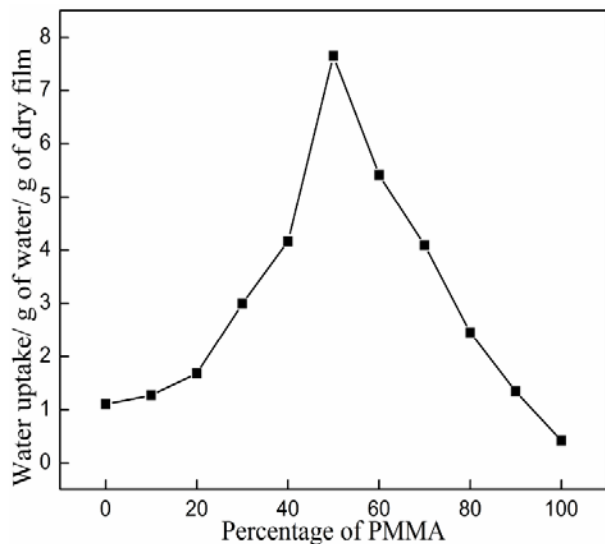


Fig 3: Water absorption by PMMA/CAP blends.

The water uptake of the blends increased upto 50 wt% of PMMA concentration. For the blend with 50 wt% PMMA, the maximum water uptake of 7.65% was observed, and the water absorption decreased on addition of further amounts of PMMA. In general, an increase in water uptake indicates the presence of voids in the polymer structure. The increase in water uptake in the blends up to 50 wt% of PMMA indicates that the blends are being formed with gradual increase in the voids in the blends. The film appears slightly cloudy after water absorption. The cloudy appearance is maximum in the case of 50% CAP blend film. The maximum amount of void spaces in the structure of the blend is formed at this composition. The hydrogen bonding between the components of the blends at this composition may be aiding this specific feature. The component polymers, at other compositions, may be blending in a gradually more compact structured pattern with the reduction in void volumes and thus reducing the water absorption.

4.4 Ion exchange capacity measurements

Ion exchange capacity (IEC) provides an indirect approximation for the ion exchangeable groups

present in the pure and blend polymers which are responsible for proton conduction. The IEC values for the PMMA/CAP blends are shown graphically in Figure 4.

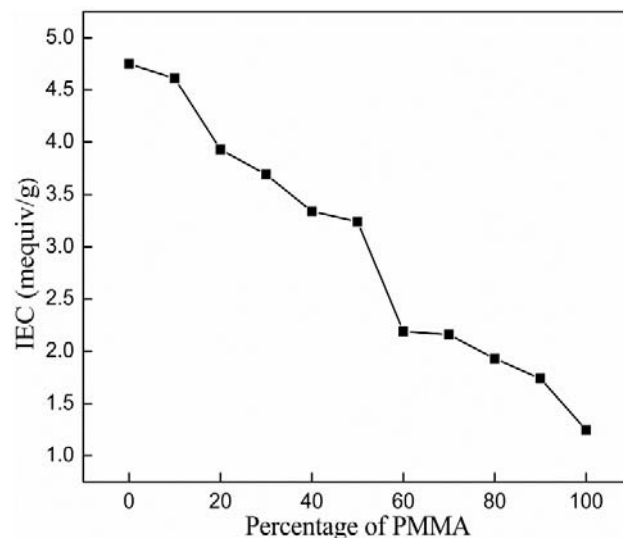


Fig 4: The change of IEC values in the PMMA/CAP blends.

From the Figure it can be seen that the IEC values of the blends decrease as the PMMA contents are increased. It is known that CAP has exchangeable $-OH$ groups. Hence it is evident that when PMMA content of the blend is increased, the number of replaceable sites available in the blend would decrease and hence the decrease in the IEC of the blends.

4.5 Electrochemical impedance spectroscopic studies

Electrochemical impedance spectroscopy is recently being widely applied in determining various material properties, prime among which are permittivity and conductivity. Figure 5 shows AC impedance spectra (Cole-Cole or Nyquist plots) of 50/50 PMMA/CAP blend at different temperatures. The impedance responses are typical of the electrolytes where the bulk resistance is the major contribution to the total resistance and minor contribution from grain boundary resistance. The straight lines inclined towards the real-axis representing the electrolyte electrode double layer capacitance behavior are

obtained for all the samples over the whole range of frequency evaluated.

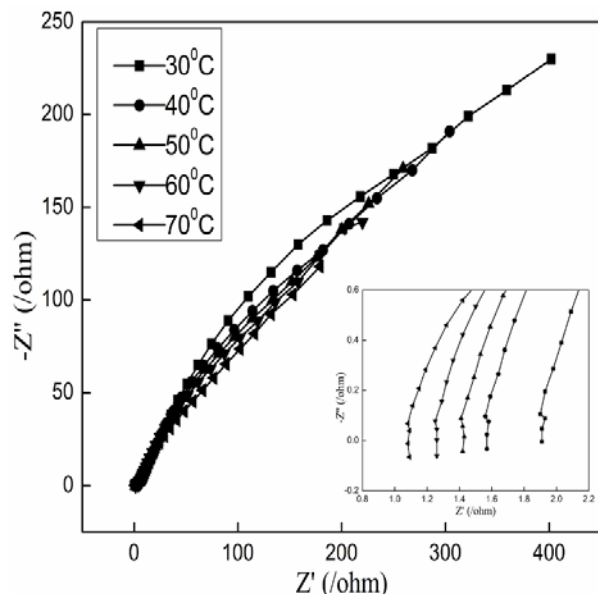


Fig 5: AC impedance spectra of 50/50 PMMA/CAP blend at different temperatures.

4.5.1 Proton conductivity measurement

The variation of conductivity of the blends with temperature and room temperature conductivity of the blends are shown in Figure 6(a) and Figure 6(b) respectively.

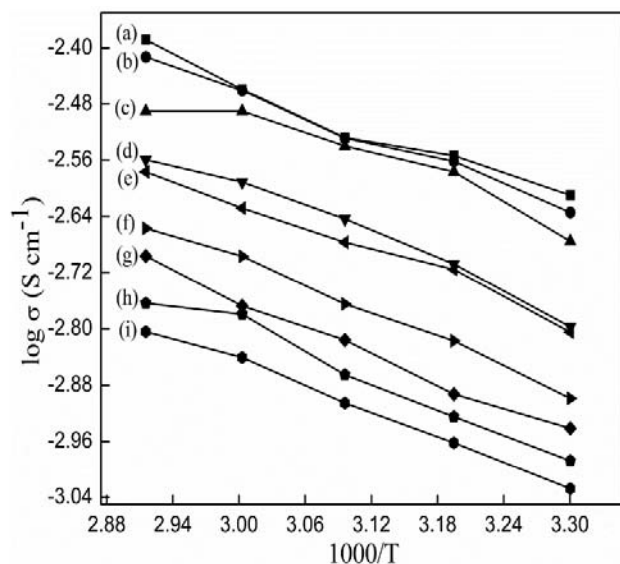


Fig 6(a): Arrhenius plots for conductivity σ of (a) 10/90, (b) 20/80, (c) 30/70, (d) 40/60, (e) 50/50, (f) 60/40, (g) 70/30, (h) 80/20, (i) 90/10 PMMA/CAP blends.

Observation has shown that at 30 °C, among the polyblends the blend with PMMA/CAP 10/90 composition showed the highest proton conductivity value of $2.46 \times 10^{-3} \text{ Scm}^{-1}$.

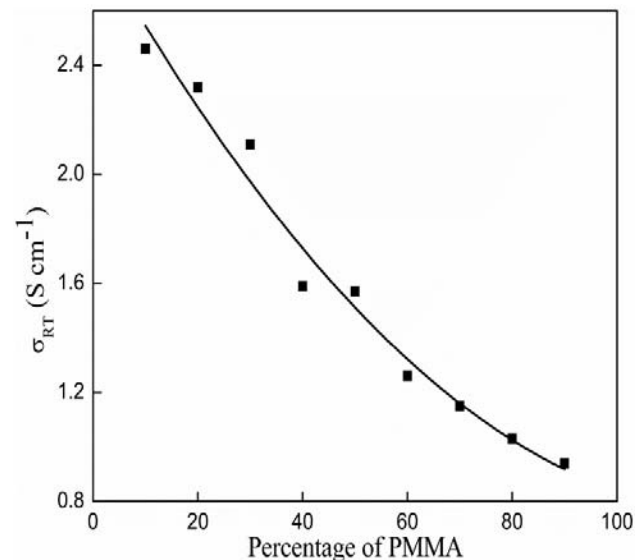


Fig 6(b): Room temperature conductivity values of PMMA/CAP blends.

The proton conductivity increased as the temperature is increased and the measured temperature range was between 30 °C to 70 °C. Furthermore, it has been found from impedance plots that as the temperature is increased, the bulk resistance R decreased resulting in an increase in the value of proton conductivity (Figure 5 inset). This may be primarily due to the fact that at higher temperature, there is an enhancement in the ion movement which favors conductivity.

4.5.2 Temperature dependence of ionic conductivity

It has been observed that the proton conductivity of the blend films increases with increase in temperature for all the compositions. This may be primarily due to the fact that an increase in temperature increases the mobility of ions which favors the conductivity. Furthermore, the conduction of ions is facilitated by the the vibrational motion of the polymer backbone and side chains, which becomes more vigorous with increase in temperature. The increased amplitude of vibration brings the coordination sites closer to

one another enabling the ions to hop from the occupied site to the unoccupied site with lesser energy required. Increase in amplitude of vibration of the polymer backbone and side chains can also increase the fraction of free volume in the polymer electrolyte system [21]. Druger et al. [22,23] have attributed the change in conductivity with temperature in solid polymer electrolyte to hopping model, which results in an increase in the free volume of the system. The hopping model either permits the ions to hop from one site to another or provides a pathway for ions to move. In other words, hopping model facilitates translational motion of the ions. Thus, it is clear that the ionic motion is due to translational motion/hopping facilitated by the polymer. Thus, the existence of overall amorphous region is indicated by the non-existence of any unusual variation of conductivity. This implies that coupling of the ion movement with the amorphous nature of the polymer is facilitating the conductivity in the blends.

Electrical conduction is a thermally activated process and follows the Arrhenius law

$$\sigma = \sigma_0 \exp\left[-\frac{E_a}{kT}\right] \quad (9)$$

where, σ is the conductivity at a particular temperature, σ_0 is the pre-exponential factor, k is the Boltzmann's constant and T is the absolute temperature. As there is no sudden change in the value of conductivity with temperature it may be inferred that these blends do not undergo any phase transitions within the temperature range studied. The variation of conductivity of the studied blends with composition at room temperature shows that conductivity increased with increase in CA content in the blends. The overall trend is similar to that of IEC variation of the blends. A steep change in conductivity of the blends in the middle range of composition is also observed which is unlike that of IEC variation. It may be recalled here that the water uptake behaviour also showed a different pattern in this region of composition. Hence the observed conductivity pattern of the blends may be

attributed to the combined effects formation of specific structural features due to hydrogen bonding and variation of exchangeable group content in the blends which are facilitating the ion hopping through the polymer structure.

4.6 Dielectric studies

The conductivity behavior of polymer electrolyte can be understood from dielectric studies [24]. The dielectric constant is a measure of stored charge. The variations of dielectric constant and dielectric loss with frequency at different temperatures have been shown in Figure 7(a) and Figure 7(b) respectively.

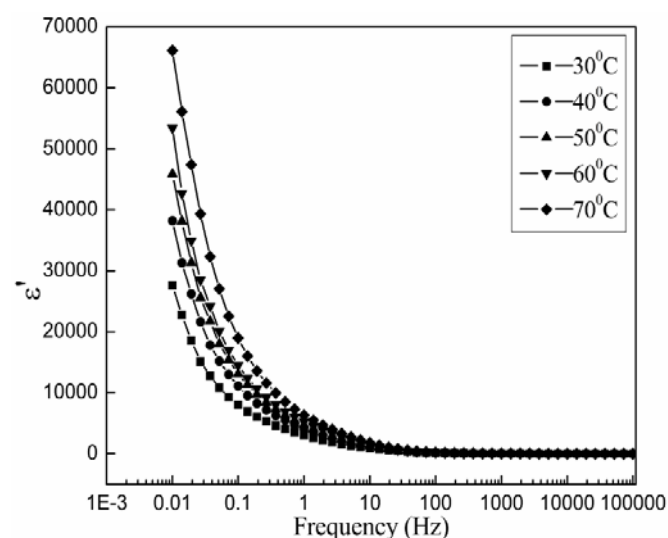


Fig 7(a): Variations of dielectric constant with frequency at different temperatures for 50/50 PMMA/CAP blend.

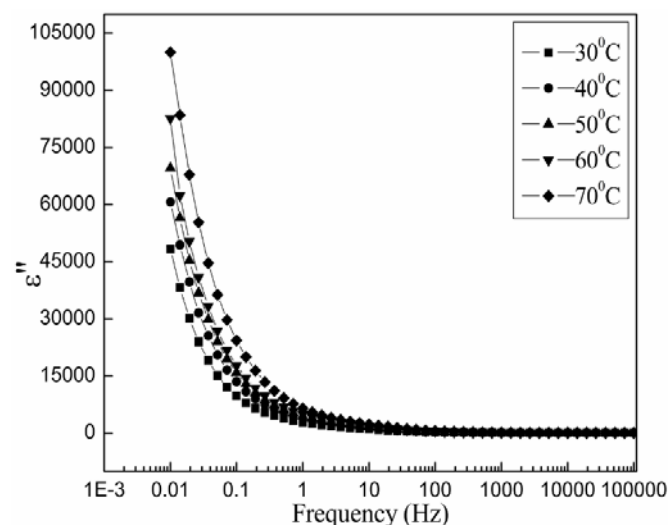


Fig 7(b): Variations of dielectric loss with frequency at different temperatures for 50/50 PMMA/CAP blend.

In this study, there are no appreciable relaxation peaks observed in the frequency range employed. Both dielectric constant and dielectric loss rise sharply at low frequencies indicating that electrode polarization and space charge effects have occurred confirming non-debye dependence [25,26]. On the other hand, at high frequencies, periodic reversal of the electric field occurs so fast that there is no excess ion diffusion in the direction of the field. Polarization due to charge accumulation decreases, leading to the observed decrease in dielectric constant and dielectric loss [27]. The dielectric constant and dielectric loss increase at higher temperatures due to the higher charge carrier density. As temperature increases, the degree of salt dissociation and redissociation of ion aggregates increases resulting in the increase in number of free ions or charge carrier density.

5. Conclusions

The PMMA/CAP blends have been prepared by solution casting method. Homogeneous polymer blend films are formed in the entire range of blend compositions and a single glass transition temperature is observed for each of the blends. FTIR-ATR and DSC results suggest that these blend systems are miscible. The miscibility of the system may be due to the formation of a hydrogen bond between the carbonyl group of PMMA and the free hydroxyl group of CAP.

The water uptake of blends increased with increasing PMMA content, whereas ion exchange capacity decreased with an increase in PMMA content. The trends in water uptake of the blends suggest the existence of inter molecular hydrogen bonding interactions between hydroxyl and carbonyl groups of CAP and PMMA respectively. These specific interactions are considered to be responsible for continuous variation in water uptake in these blends. The variation in ion exchange capacity of the blends indicated that this property is mainly governed by the exchangeable group content present in the blends.

The maximum proton conductivity obtained at room temperature was $2.46 \times 10^{-3} \text{ S cm}^{-1}$ for PMMA/CAP 10/90 blend. The proton

conductivity in these films has been attributed to the operation of hopping model type of mechanism. The dielectric studies of the blends suggest the absence of relaxation phenomenon. These materials may also be used as bioblends.

6. Acknowledgements

H.S. Sreekantha Jois is grateful to NITK Surathkal for the award of a research fellowship.

7. References

1. Ramesh SAH, Yahaya AK. Arof. Miscibility studies of PVC blends (PVC/PMMA and PVC/PEO) based polymer electrolytes. *Solid State Ionics* 2002; 148:483-486.
2. Peesan MP, Supaphol, R. Rujiravanit. Effect of casting solvent on characteristics of hexanoyl chitosan/poly lactide blend films. *J Appl Polym Sci* 2007; 105:1844-1852.
3. Prusty M, Keestra BJ, Goossens JGP, Anderson PD. Experimental and computational study on structure development of PMMA/SAN blends. *Chem Eng Sci* 2007; 62:1825-1837.
4. Kumaraswamy GN, Ranganathaiah C, Urs MVD, Ravikumar HB. Miscibility and phase separation in SAN/PMMA blends investigated by positron lifetime measurements. *Eur Polym J* 2006; 42:2655-2666.
5. Adoor SG, Manjeshwar LS, Rao KSVK, Naidu BVK, Aminabhavi TM. Solution and solid-state blend compatibility of poly (vinyl alcohol) and poly (methyl methacrylate). *J Appl Polym Sci* 2006; 100:2415-2421.
6. Kuo SW, Chang FC. Studies of miscibility behavior and hydrogen bonding in blends of poly (vinylphenol) and poly (vinylpyrrolidone). *Macromolecules* 2001; 34:5224-5228.
7. Kuo SE, Tung PH, Chang FC. Syntheses and the study of strongly hydrogen-bonded poly (vinylphenol-*b*-vinylpyridine) diblock copolymer through anionic polymerization. *Macromolecules* 2006; 39:9388-9395.
8. Elashmawi IS, Hakeem NA, Abdelrazek EM. Spectroscopic and thermal studies of PS/PVAc blends. *Physica B: Physics of Condensed Matter* 2008; 403:3547-3552.
9. Jois HSS, Bhat DK. Miscibility, water uptake, ion exchange capacity, conductivity and dielectric studies of poly (methyl methacrylate) and cellulose acetate blends. *J Appl Polym Sci* 2013; 130(5):3074-3081. DOI: 10.1002/app.39535.
10. Selvakumar M, Bhat DK, Renganathan NG. Miscibility of polymethylmethacrylate and

- polyethyleneglycol blends in tetrahydrofuran. *J Appl Polym Sci* 2009; 111:452-460.
11. Selvakumar M, Bhat DK. Miscibility of poly (vinylidene fluoride) and cellulose acetate blends in dimethyl formamide. *Asian J Chem* 2011; 23:1474-1478.
 12. Bhatt AS, Bhat DK. Influence of nanoscale NiO on magnetic and electrochemical behavior of PVDF-based polymer nanocomposites. *Polym Bull* 2012; 68:253-261.
 13. Bhatt AS, Bhat DK, Santosh MS, Tai CW. Chitosan/NiO nanocomposites: a potential new dielectric material. *J Mater Chem* 2011; 21:13490-13497.
 14. Kuo SW, Kao HC, Chang FC. Thermal behavior and specific interaction in high glass transition temperature PMMA copolymer. *Polymer* 2003; 44:6873-6882.
 15. Rosa DS, Guedes CGF, Casarin F, Braganca FC. The effect of the Mw of PEG in PCL/CA blends. *Polym Test* 2005; 24:542-548.
 16. Sahu AK, Selvarani G, Bhat SD, Pitchumani S, Sridhar P, Shukla AK, Narayanan N, Banerjee A, Chandrakumar N. Effect of varying poly (styrene sulfonic acid) content in poly (vinyl alcohol)-poly (styrene sulfonic acid) blend membrane and its ramification in hydrogen-oxygen polymer electrolyte fuel cells. *J Membrane Sci* 2008; 319:298-305.
 17. He Y, Zhu B, Inoue Y. Hydrogen bonds in polymer blends. *Prog Polym Sci* 2004; 29:1021-1051.
 18. Gordon M, Taylor J. Ideal copolymers and the second-order transitions of synthetic rubbers. i. non-crystalline copolymers. *J Appl Chem* 1952; 2:493-500.
 19. Shirahase T, Komatsu Y, Tominaga Y, Asai S, Sumita M. Miscibility and hydrolytic degradation in alkaline solution of poly (L-lactide) and poly (methyl methacrylate) blends. *Polymer* 2006; 47:4839-4844.
 20. Fox TG. Influence of diluents and of copolymer composition on the glass temperature of a polymer system. *Bull Am Phys Soc* 1956; 1:123.
 21. Aziz SB, Abidin ZHZ, Arof AK. Effect of silver nanoparticles on the DC conductivity in chitosan-silver triflate polymer electrolyte. *Physica B* 2010; 405:4429-4433.
 22. Druger SD, Nitzan A, Ratner MA. Dynamic bond percolation theory: A microscopic model for diffusion in dynamically disordered systems. I. Definition and one-dimensional case. *J Chem Phys* 1983; 79:3133-3142.
 23. Druger SD, Ratner MS, Nitzan A. Generalized hopping model for frequency-dependent transport in a dynamically disordered medium, with applications to polymer solid electrolytes. *Phys Rev B* 1985; 31:3939-3947.
 24. Ramesh S, Yahaya AH, Arof AK. Dielectric behavior of PVC-based polymer electrolytes. *Solid State Ionics* 2002; 152-153:291-294.
 25. Qian X, Gu N, Cheng Z, Yang X, Wang E, Dong S. Impedance study of (PEO)₁₀LiClO₄-Al₂O₃ composite polymer electrolyte with blocking electrodes. *Electrochim. Acta* 2001; 46:1829-1836.
 26. Govindaraj G, Baskaran N, Shahi K, Monoravi P. Preparation, conductivity, complex permittivity and electric modulus in AgI-Ag₂O-SeO₃-MoO₃ glasses. *Solid State Ionics* 1995; 76:47-55.
 27. Ramesh S, Arof AK. Structural, thermal and electrochemical cell characteristics of poly (vinyl chloride)-based polymer electrolytes. *J Power Sources* 2001; 99:41-47.